THE JOURNAL OF PHYSICAL CHEMISTRY C

ARTICLE

pubs.acs.org/JPCC

Conformational Adaptation and Electronic Structure of 2H-Tetraphenylporphyrin on Ag(111) during Fe Metalation

Giovanni Di Santo,[†] Carla Castellarin-Cudia,[†] Mattia Fanetti,[†] Bidini Taleatu,[†,§,∥] Patrizia Borghetti,[‡] Luigi Sangaletti,[‡] Luca Floreano,[¶] Elena Magnano,[¶] Federica Bondino,[¶] and Andrea Goldoni[†,*]

[†]Sincrotrone Trieste S.C.p.A. s.s.14 Km. 163.5, 34012 Trieste, Italy

[‡]Department of Physics, Università Cattolica del Sacro Cuore Brescia, Italy

[¶]Istituto Officina dei Materiali-CNR, Lab. TASC, s.s. 14 km 163,5, 34149 Trieste, Italy

[§]Department of Physics, Obafemi Awolowo University - Ile-Ife, Nigeria

[∥]International Center of Theoretical Physics, St. Costiera 11, 34151 Trieste, Italy

Supporting Information

ABSTRACT: In-situ metalation of porphyrin molecules in ultrahigh vacuum (UHV) is of great interest for the characterization of pure species in a controlled environment. Here, we report the characterization of the electronic states and the molecules' geometrical adaptation during the formation of pure 2H-5,10,15,20-tetraphenylporphyrin (2H-TPP) and Fe- tetraphenylporphyrin (Fe-TPP) layers on Ag(111) single crystal. Core level absorption spectra indicate the flat conformation of the monolayer suggesting an adatom hopping instead of a surface mediated dopant diffusion for the metalation process. Photoemission points out that the interaction between Fe d_z-states and Ag bands increases the monolayer metallic character already induced by the charge transfer from the substrate.

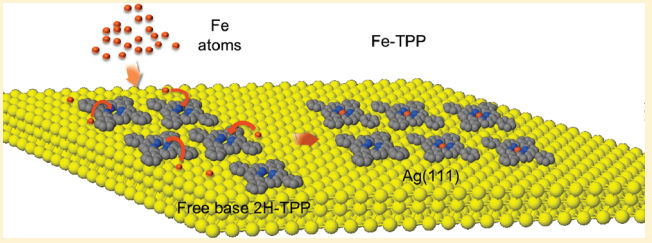

INTRODUCTION

Porphyrins represent a group of molecules with an unsaturated macrocyclic ring. The alternation of single and double bonds all through the macrocycle makes porphyrin systems chemically very stable and versatile with many positions where different functional groups can be substituted. Moreover, there is the possibility to include several kinds of metal atoms at the center of the macrocycle. Typically, the inclusion of metal atoms in porphyrin molecules is obtained via chemical reaction in solvents. The most prominent representatives of these complexes, the so-called metallo-porphyrins, are the iron-porphyrins with an Fe(II) ion complexed to the four nitrogen atoms in the center of the conjugated ring system. These molecules play a key role in several oxidative catalytic processes, including biological systems. Iron-porphyrins may undergo reversible redox reactions and are very sensitive toward oxidation.[1] Hence, they are very difficult to handle and sublimate as a pure compound. So far, the commercially available porphyrins with an Fe ion at the center of the macrocycle have also a Cl bonded to the iron to stabilize the highly reactive metal that can easily oxidize. The possibility to produce stable Fe-porphyrins with no Cl atoms and to characterize them in situ is an intriguing challenge that is of fundamental interest because of their key role as main building blocks in important biological molecules such as cytochrome P-450 and hemoglobin[2,3] as well as for magnetic systems[4] and catalytic processes.[5]

Recently, it was shown that pure Fe-tetraphenylporphyrin (Fe-TPP) can be produced under UHV conditions by in-situ metalation of free-base 2H-5,10,15,20-tetraphenylporphyrin (2H-TPP) monolayers with Fe atoms that were deposited using an electron beam evaporator.[6] In this experiment, scanning tunneling microscopy (STM) micrographs with submolecular resolution were presented showing the appearance of intramolecular protrusions consequent to Fe evaporation. These protrusions have been taken as the evidence of the TPP metalation. Similar experiments have been performed for Co and Ce.[7] Moreover, photoemission studies, performed with laboratory X-ray sources, have demonstrated metalation by Fe, Zn, and Co of free-base porphyrins by collecting the N 1s core level signal together with the metal peak.[8−10] Metalation experiments were also performed on free-base phtalocyanines.[11] The above studies demonstrated that metals can efficiently be coordinated with adsorbed porphyrin and phtalocyanine layers by in-situ evaporation of metal atoms under clean UHV conditions. This approach represents a possible route toward the production of porphyrin

Received: November 22, 2010
Revised: January 10, 2011
Published: February 22, 2011

materials not yet available or not easily obtainable using the simple and energetically favorable capabilities of a metal-to-molecule direct coordination[12] as well as the ability to access for low-dimensional metal−organic architectures and patterned surfaces, which cannot be achieved with other conventional methods. Therefore, the complete understanding of the coordination mechanisms is of straightforward interest.

Although there are several studies on this subject, in particular related to Fe metalation, the models of the molecular structural configuration and adaptation on the substrate surface need to be refined and the studies in the single layer should be clarified from the core level spectroscopy point of view before and after the metalation. In particular, much less attention was devoted to the interface adsorption geometry and the multilayer molecular orientation. The possible distortion of the macrocycle and how the electronic structure will change after the metalation has never been checked in detail. Moreover, on the basis of both experimental and theoretical data, the monolayer metalation process was explained with the diffusion of the metal at the reaction site driven by motion onto the substrate surface;[8,13−15] however, this model seems inadequate for phtalocyanine overlayers, which form a compact wetting layer, covering the whole substrate.[11]

The aim of this work is to add direct information on the geometry of the 2H-TPP monolayer and of the multilayer as well as to point out the electronic features that support the substrate−molecule interaction. By means of high-resolution photoemission spectroscopies from core level and valence band states (X-ray photoelectron spectroscopy, XPS) and near edge X-ray absorption fine structure (NEXAFS) spectroscopy, performed with synchrotron radiation source, we evaluate the Fe complexes' formation, and we characterize the electronic structure of the specimens when passing from 2H-TPP to Fe-TPP in both the monolayer and the multilayer.

EXPERIMENTAL SECTION

The data were collected at ALOISA (NEXAFS) and BACH (Photoemission) beamlines at the Elettra Synchrotron Radiation facility in Trieste. All the experiments were performed in UHV experimental chambers at a base pressure of 10^{-10} mbar. Highly purified (99.95%) commercial 2H-TPP powder was used, and the molecules were sublimated at 570 K directly on Ag(111) kept at room temperature by a homemade, resistively heated, Ta evaporator. The Ag(111) surface was prepared by Ar^+ sputtering at 1 keV and annealing at 700 K. The absence of contaminants and the ordering of the surfaces were checked by means of XPS, reflective high energy electron diffraction (RHEED), and low-energy electron diffraction (LEED) techniques. The 2H-TPP monolayers (ML) were obtained by sublimating a predeposited thick film of 2H-TPP molecules at ∼530 K. We therefore define 1 ML of 2H-TPP as the maximum coverage of molecules adsorbed on the substrate surface after the above procedure. Fe atom evaporation was made by means of a highly focused electron bombardment evaporator (Omicron). After each Fe evaporation, the substrate was annealed at ∼400 K for enhancing the metal diffusion. No irradiation damage was observed for the monolayer irrespective of the exposure time. On thick films, slight changes of the stoichiometric ratio between the nitrogen iminic and the pyrrolic components were observed (photoemission) after long-time exposures (hours), much longer than the acquisition time for the present data. We therefore repeated the film deposition and, consequently, the Fe evaporation after each set of measurements.

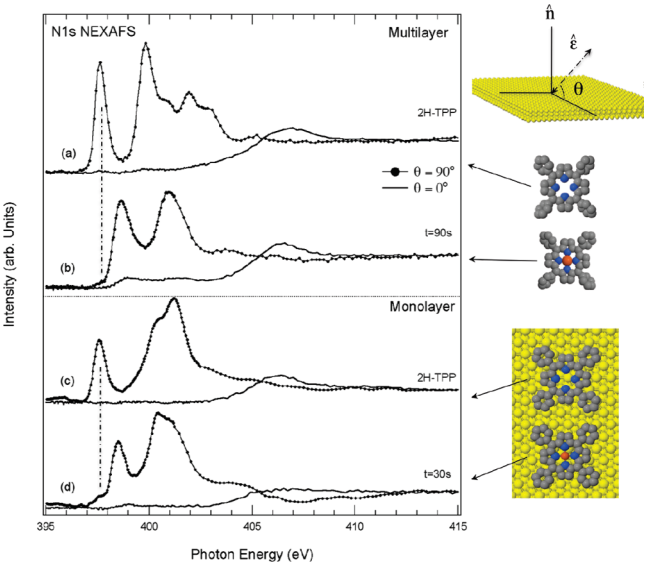

Figure 1. NEXAFS spectra at the N 1s threshold for multilayer (a, b) and monolayer (c, d). The spectra are taken in linear s-polarization (θ = 0°) and in p-polarization (θ = 90°).

NEXAFS spectra were taken in partial electron yield by means of a channeltron facing the sample while scanning the photon energy across the C and N K-edge with an energy resolution of 100 meV.[16] The low-energy secondary electrons were filtered out by means of a negatively polarized grid (−230 V for the carbon edge, −370 V for the nitrogen edge) placed in front of the sample. The orientation of the surface with respect to the linear polarization of the synchrotron beam was changed by rotating the sample around the beam axis while keeping a constant grazing angle of 6°.[17] This scattering geometry allows the change from linear s-polarization (θ = 0°) to p-polarization (θ = 90°) without variation of the illuminated area on the sample. The raw data were normalized to the total photon flux.

The XPS data for TPP molecules on Ag(111) were collected by means of a hemispherical electron energy analyzer VSW CLASS 150. The analyzer is at 60° from the incident photon beam in the horizontal plane. The photoemission measurements were collected with a ±4° angular acceptance with a photon energy of 175 and 530 eV[18] and a total resolution of 150 and 360 meV, respectively. The binding energies (BEs) of the photoemission spectra were calibrated using the Fermi level of Ag(111).

RESULTS AND DISCUSSION

Adsorption Orientation and Conformation. We have used the dependence of NEXAFS from the linear polarization of the light to investigate the electronic transitions from core levels to empty states and to determine the adsorption geometry of 2H-TPP deposited on Ag(111) in the monolayer and multilayer cases. In Figure 1a, c and Figure 2a, c we report the NEXAFS spectra at the N and C K-edges for the 2H-TPP deposited on the Ag(111) substrate, respectively, for the angles θ = 0° and θ = 90° between the linear light polarization and the surface plane. The spectra were normalized to the total photon flux intensity and, according to the procedure indicated in ref 19, were normalized at the σ^* states at high-photon energy after a pre-edge baseline

dx.doi.org/10.1021/jp111151n |J. Phys. Chem. C 2011, 115, 4155–4162

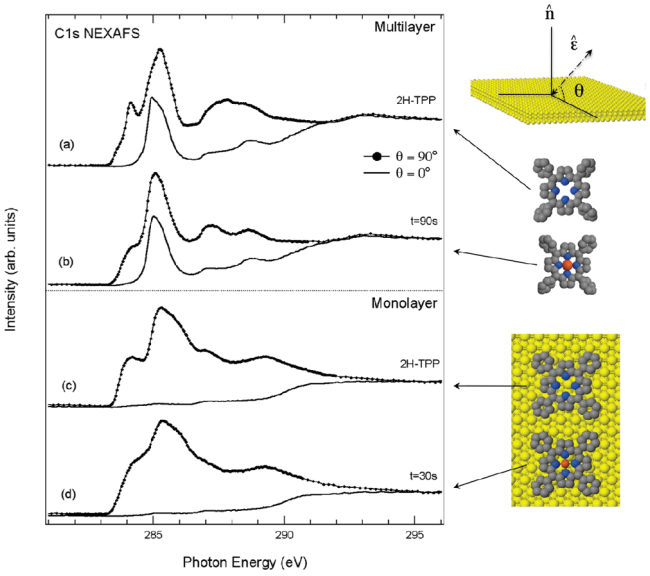

Figure 2. NEXAFS spectra at the C 1s threshold for multilayer (a, b) and monolayer (c, d). The spectra are taken in linear s-polarization (θ = 0°) and in p-polarization (θ = 90°).

subtraction. In general, the π^* states that characterize planar organic aromatic molecules consist of a contribution that mainly belongs to a combination of atomic-like p_z orbitals, which lie perpendicular to the plane containing the aromatic frame. This is the case of porphyrin: in particular, the π^* generated by the four central nitrogen atoms are well separated in energy from the remaining empty orbitals, therefore, they are easy to study and will give a clear indication on the molecular empty states and on the orientation of the molecular skeleton with respect to the supporting surface.[19] Figure 1a shows the N K-edge NEXAFS spectrum of the 2H-TPP multilayer. This spectrum is similar to the 2H-TPP gas-phase spectrum, indicating that the interaction between the molecules is weak (see Supporting Information). Peaks at photon energies smaller than 404 eV are π^* resonances, and for their assignment, we refer to a former study by Polzonetti.[20] From the comparison between the spectra taken with the light polarization parallel (θ = 0°) and perpendicular (θ = 90°) to the surface, it is possible to extract the information about the geometry of the system. In this case, we see a complete quenching of the π^* states at θ = 0°, indicating a flat adsorption configuration for the macrocycle.

The analysis of the absorption spectra measured at the C 1s (Figure 2 a) threshold put in evidence the geometry assumed by the whole molecule, in particular, by the phenyl rings with respect to the substrate and the macrocycle. The first two structures belonging to the peak at $h\nu \sim 284$ eV are assigned to the macrocycle, while the huge absorption structure at $h\nu \sim 285$ eV is mainly due to the π^* states located in the phenyl groups.[21] As in the case of the N 1s threshold, the macrocycle peak disappears at θ = 0° (first π^* transition), indicating again that the macrocycle stays flat with respect to substrate surface plane, but the huge phenyl π^* peak is still present, thus indicating a nonflat orientation of the meso-substituent rings. This is not unexpected since the phenyl rings in the isolated molecules tend to stay at approximately 70−80° with respect to the macrocycle because of the hydrogen steric interactions. In the multilayer, the intermolecular forces are mainly van der Waals; therefore, the coupling among the constituent molecules

Table 1. Multilayer of Fe-TPP Complex Formation on Ag-(111): Normalized Intensity and BE N 1s Components

evaporation step	normalized peak areas		
	−N=	−NH−	NFe
no Fe (TPP only)	0.42	0.58	
first (t_{evap} = 30 s)	0.22	0.33	0.45
second (t_{evap} = 60 s)	0.16	0.23	0.61
third (t_{evap} = 90 s)	0.09	0.13	0.78
BE (eV)	397.9	399.9	398.6

Table 2. Monolayer of Fe-TPP Complex Formation on Ag(111): N 1s Components Normalized Intensity, D−S Asymmetry Parameter, and BE

evaporation step	normalized peak areas			α
	−N=	−NH−	NFe	
no Fe (TPP only)	0.52	0.48		0.11
first (t_{evap} = 10 s)	0.28	0.26	0.46	0.13
second (t_{evap} = 20 s)	0.075	0.065	0.86	0.19
third (t_{evap} = 30 s)			1.0	0.21
BE (eV)	397.7	399.7	398.4	

is faint and the phenyl meso-substituents should be oriented in a way akin to the isolated molecules. On the contrary, the monolayer showed a flat molecular adsorption geometry with a planar conformation for the phenyl groups as clearly seen from the suppression of all the π^* peaks at θ = 0° in the N 1s and C 1s NEXAFS spectra (Figure 1c and Figure 2c). Therefore, the procedure for obtaining the monolayer and the molecule−substrate interaction appear to be strong enough to force a change in the molecule and to win in some way the hydrogen steric forces in order to have the phenyl groups in a planar geometry. A similar flat arrangement of both macrocycle and phenyl legs has been observed also for ZnTPP on Ag(110)[21] and for 3,5-di-tert-butylphenyl-porphyrin (TBPP) on Cu(111),[22,23] but it has never been reported for Ag(111). In fact, STM experiments and density functional theory (DFT) calculations seem to demonstrate that the molecules adsorb with a nonzero aryl angle. We demonstrate in another publication that the annealing at 530 K for the preparation of the 2H-TPP monolayer results in a chemical modification of the porphyrin allowing a flat conformation of the molecules.[24] The flat rotation of the benzene rings on the substrate surface enables a rather strong chemical interaction between the π states of the carbon atoms and the s−p bands of silver.

The molecular adsorption should give rise to an interface dipole with a decrease of work function of the underlying metal and a net charge transfer to the adsorbate layer as indicated by the rigid shift of −0.2 eV of the N 1s BE as measured in the monolayer with respect to the multilayer (see Table 1 and Table 2). The charge transfer modifies the energy-level alignment (i.e., the molecules' distance from the substrate surface), and it is due to a competition between the molecular conformation and the adsorbate self-assembly driving force. The strong interaction and the conformation observed lead to a high adsorption energy. In fact, above 600 K, the monolayer molecules start to decompose, and it is not possible to desorb the intact monolayer molecules.

dx.doi.org/10.1021/jp111151n |J. Phys. Chem. C 2011, 115, 4155–4162

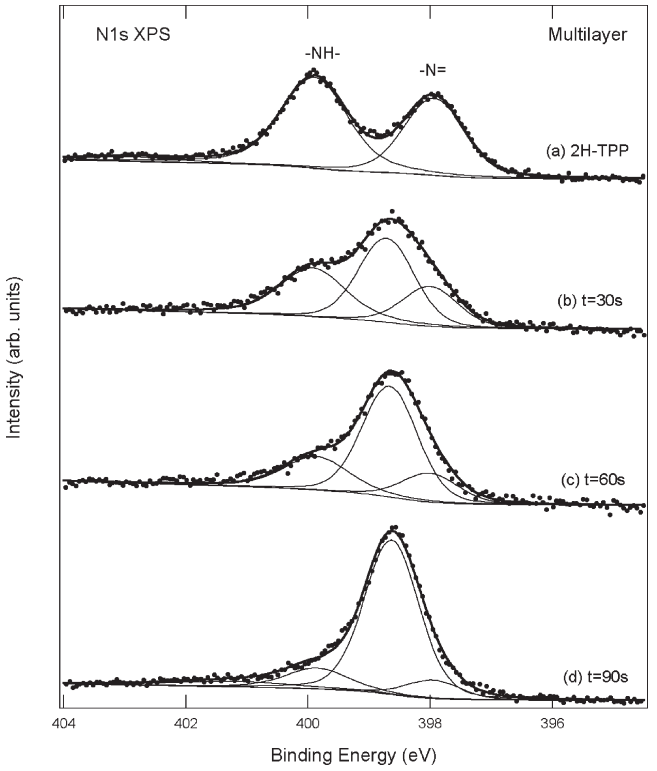

Figure 3. N 1s XPS spectrum of 2H-TPP multilayer before and after Fe deposition steps. The used photon energy was $h\nu$ = 530 eV. The formation of the peak at BE = 398.6 eV gives evidence of the N−Fe coordination.

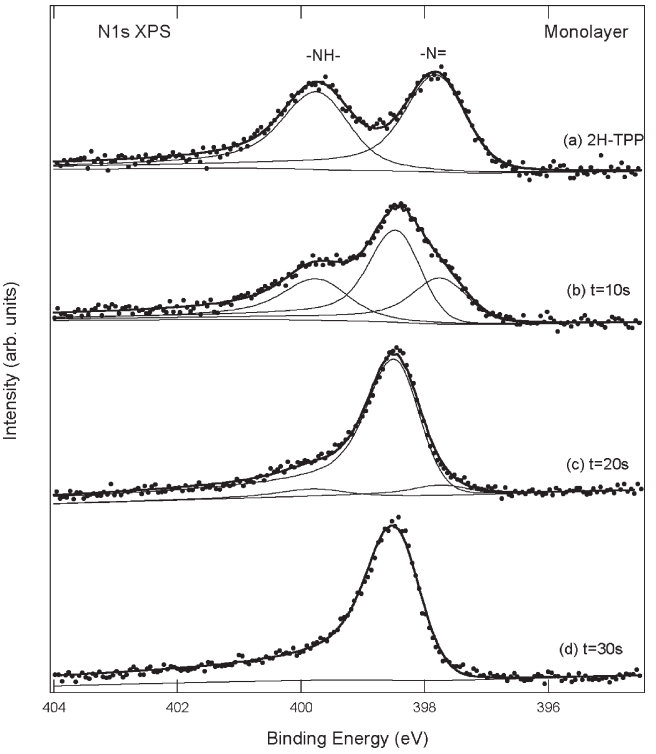

Figure 4. N 1s XPS spectrum of 2H-TPP monolayer before and after Fe deposition steps. The used photon energy was $h\nu$ = 530 eV. The formation of the peak at BE = 398.4 eV gives evidence of the N−Fe coordination.

Fe Metalation. X-ray photoemission spectra provide the straightforward evidence of the Fe coordination. In particular, the N 1s spectrum of the porphyrin is expected to change when the iron is bound at the center of the macrocycle. In fact, the N 1s spectrum of 2H-TPP has two easily resolved components because of the two N species (iminic and pyrrolic), whereas the N atoms are equivalent in Fe-TPP, and just one peak is expected.

In fact, the 2H-TPP spectra for multilayer and monolayer, reported in Figure 3a and Figure 4a, are composed by two peaks: the one at higher binding energy is assigned to the two pyrrolic N atoms (−NH−), while the lower BE peak corresponds to the two iminic ones (−N=).[25] The BE values obtained by fitting the spectra are in good agreement with similar results already reported in the literature[10] and are reported in Table 1 and Table 2. The immediate deduction, looking at Figure 3a, is that the pyrrolic peak is broader than the iminic. The multilayer fit procedure was made using a Shirley background and Voigt integral functions. Using the same Gaussian function, the best fit returned a Gaussian with a full width at half-maximum (fwhm) of 0.65 eV convoluted with Lorentzian peaks associated to the two N atom components. The values for Γ_N and Γ_{NH} (Lorentzian width) are 0.74 eV and 0.88 eV, respectively. However, it is difficult to assert that the two kinds of N 1s atoms, with such a Γ difference of 0.14 eV, have a different core-hole lifetime that should be related to very distinct de-excitation mechanisms. The core-hole de-excitations are mainly due to Auger transitions and, therefore, are controlled by the Coulomb matrix elements that might hardly be different in the two cases. On the other hand, the presence of two nitrogens bonded with H introduces more phonon modes related to the N−H bond vibrations,[26] which can be expected to broaden the pyrrolic peak because of a Franck−Condon mechanism in the photoemission process. The unresolved phonon fine structure in the measured peak can be effectively taken into account by considering a Gaussian broadening of the core level line width. Therefore, we made a second fit by assuming that both nitrogen components have the same Γ width and by changing the Gaussian fwhm. This gives a Γ = 0.84eV and the two fwhm's equal to 0.655 eV and 0.590 eV for the pyrrolic and the iminic peaks, respectively.

The normalized peak areas, listed in Table 1, show clearly an uneven proportion of the two N components. We explain the small disproportion between the two N components with a photoelectron diffraction effect. Indeed, in our experimental geometry, the ordering of the molecular layer should enhance the photoelectron diffraction modulation (electrons are collected at $\theta = 60°$ with respect to surface normal).

Since core level spectroscopy experiments extract information on the electronic structure, the comparison between NEXAFS and XPS and their data analysis is able to clarify the electrical character of the molecular film. As expected from the NEXAFS N 1s spectrum of Figure 1a, we observe that the first two π^* transitions correspond to the two peaks visible in photoemission, indicating that an electron transition from both of two nonequivalent N 1s core levels into the same empty state is allowed. When we take a closer look at the energy positions, we notice that the first π^* peak is shifted toward lower energies by 0.3 eV with respect to the corresponding XPS BE. This generally happens for a semiconducting system, and it is due to Coulomb interaction between the core-hole and the excited electron.

In the following, the metallization of the multilayer is analyzed. In this case, the multilayer corresponds to approximately four layers as estimated from the attenuation of the Ag 3d signal. Such a thin layer should guarantee the possibility to follow the Fe metalation of the TPP overlayer in a reasonable experimental time. As already said, the evidence of the in situ complex formation comes from the N 1s spectra taken before and after the Fe evaporation. In Figure 3, we show that the sequence of the N 1s line shape changes during Fe evaporation. The two inequivalent nitrogen components (separated by 2 eV) present in the macrocycle are reduced to a single component while the Fe atoms are evaporated and react with the deposited porphyrin multilayer. The N 1s spectrum changes toward a single peak configuration, which corresponds to four equivalent nitrogen atoms in the macrocycle, all unprotonated and coordinated with a single Fe atom. By fitting these core levels, we found the pyrrolic peak (−NH−) at BE = 399.9 eV, the iminic N one (−N=) at BE = 397.9 eV, and the peak corresponding to the N−Fe bond at BE = 398.6 eV.

As it is shown in Figure 3, the metalation of the multilayer film is almost complete, since the area corresponding to the N−Fe component is 78% of the total. The Fe atom coordination at the center of the porphyrin macrocycle, evidenced from photoemission measurements, is confirmed by the N 1s absorption spectra (Figure 1 b). For example, the first two π^* peaks of the 2H-TPP NEXAFS spectrum are converged to a single peak located at a photon energy of $h\nu$ = 398.6 eV (Figure 1 b). The presence of a small shoulder at lower energy confirms that not all of the molecules have been metalated. The π^* states at higher photon energies (>400 eV) are also related to the macrocycle, and their changes after the metal evaporation can be associated with the Fe coordination. In particular, the whole Fe-TPP NEXAFS spectrum seems like that of Ni−TPP,[27] further suggesting the bonding of Fe atoms at the center of the macrocycle.

From Figure 1b, we notice that the NEXAFS peak at 398.6 eV is not completely quenched when the polarization is in the surface plane ($\theta = 0°$). Even if no clear peaks are visible at $\theta = 0°$, the presence of this feature suggests that, in the Fe-TPP multilayer, the four nitrogen atoms slightly change their orientation because of the Fe atom coordination. On the other hand, looking at the C 1s NEXAFS (Figure 2b), it is evident that the macrocycle carbon atoms have not changed their orientation. This distortion of the planar configuration, seen for the nitrogen and missing in the case of carbon, indicates the unchanged macrocycle orientation with a possible distortion of the N positions.[28]

Differently from the 2H-TPP, in the metalated case (Figure 1b), the first transition appears at the exact BE of the corresponding photoemission core level. This is typical for a metallic or quasi-metallic-like behavior as the Coulomb interaction is screened by conduction electrons.

The same experiment done for the multilayer has been reproduced for one monolayer. We define the monolayer as the saturated layer obtained by multilayer desorption. Since the monolayer displays a flat configuration, as evidenced by NEXAFS results, the estimated coverage of the clean unreconstructed Ag(111) surface by our XPS measurements for the monolayer is about one 2H-TPP molecule (44 C and 4 N atoms) every 27 Ag atoms.[6] This is in agreement with other determinations of the saturated 2H-TPP monolayer on Ag(111) and gives a reliable way to estimate quantitatively the amount of Fe deposited. Moreover, it is also clear, taking into account the atomic photoionization cross sections, how the Ag signal is predominant in the overall XPS spectrum and how a large counting statistic is required to highlight the N 1s spectrum features. In fact, the Ag 3d plasmon strongly modifies the XPS background in the N 1s region, and the Ag 3s peak almost superimposes on the Fe 2p.

The monolayer XPS peak positions rigidly shift toward lower binding energy by 0.2 eV with respect to the multilayer case (a similar shift is observed for the C 1s), and this is related to the surface dipole formation by substrate electrons being transferred and by the better screening of the core hole because of the underlying metal. The N 1s core-level fit has been performed in agreement with the same procedure used for the multilayer. In addition, the N peaks clearly show a certain degree of asymmetry as expected for metallic systems. This can be explained in the first place with a strong interaction of the molecule with the metallic substrate which is further emphasized by the presence of the Fe atoms. For this reason, the best fit to monolayer data has been done using Doniach−Sunjic[29] functions, that is, integral expressions taking into account the peak asymmetry in the photoemission process related to the electronic transitions at very small energy across the Fermi level for metallic systems. As in the case of the multilayer, we recognize that the peak width of the two components is different, and accordingly, we fitted the data assuming the same Lorentzian width (Γ) and changing the Gaussian fwhm. The obtained values are Γ = 0.50 eV, and the fwhm's are 0.77 eV and 0.80 eV for the iminic and the pyrrolic peak, respectively. A clear increase in the asymmetry parameter (α), as the Fe complexation takes place, is also visible and is reported in Table 2. According to the area values listed in Table 1 and Table 2, we reckon that, as expected, there is a minor photoelectron diffraction effect for the monolayer with respect to the multilayer in this adsorption geometry.

The metalation procedure has led to an almost fully metalated ML, as shown by the single peak of the N 1s spectrum (Figure 4d), with an evaporation of 0.030 ± 0.005 ML of Fe (about 1 Fe atom every 4.9 ± 0.5 N atoms). However, the spectra taken in the Fe 2p region for the full Fe-TPP monolayer formation show a very small structure hardly distinguishable from the background because of the unavoidable presence of the Ag 3s signal. Related data on the Fe 2p region are not included in the manuscript but are available in the Supporting Information.

For the NEXAFS spectrum, we have repeated the iron evaporation procedure on a new ML. In this case, the ML metalation was not complete as shown by the small pre-edge feature in Figure 1d. The N 1s NEXAFS, shown in Figure 1c, of the 2H-TPP ML presents the first π^* absorption peak at $h\nu$ = 397.7 eV as the BE of the N 1s iminic component measured in photoemission. The correspondence with the photoemission BE is found also for the first π^* transition (Figure 1d) in the case of a fully metalated TPP. Again, this agrees with the metallic behavior of the monolayer (both 2H-TPP and Fe-TPP) as shown by core level XPS and, as we will discuss later on, by valence band data. Moreover, the monolayer adsorption orientation and conformation are still controlled through the coupling of phenyl legs to the substrate. The flat conformation of phenyl legs for the monolayer simultaneously predefines the relative molecular orientations and reduces the degrees of freedom for the Fe complex formation toward the already reached lowest energy situation.[24] The influence of the Fe metallic center in the porphyrin core has only minor effects for the geometry of the macrocycle in the monolayer case.

Finally, our metalation results on the monolayer are in perfect agreement with those obtained by Bai et al. for phtalocyanine

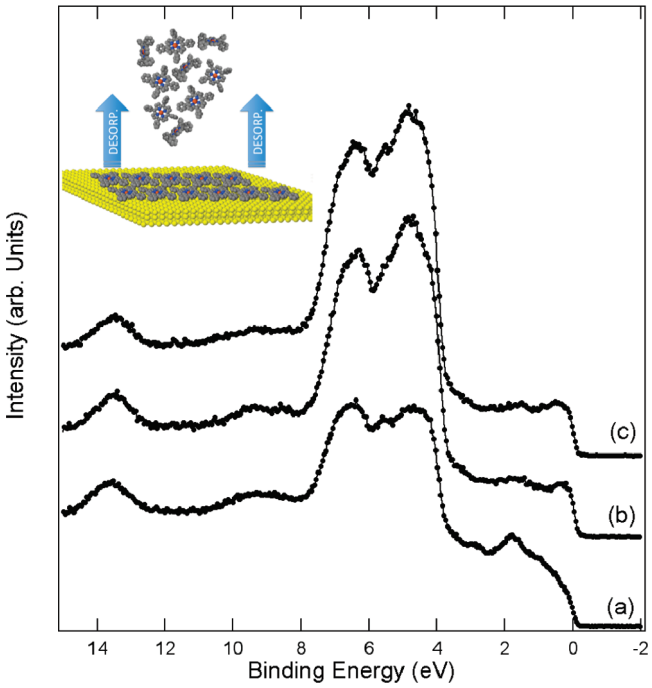

Figure 5. Raw data valence band spectra of (a) an Fe-TPP multilayer and (b) the corresponding ML and (c) the ML obtained by desorption of the multilayer . The used photon energy was $h\nu$ = 175 eV.

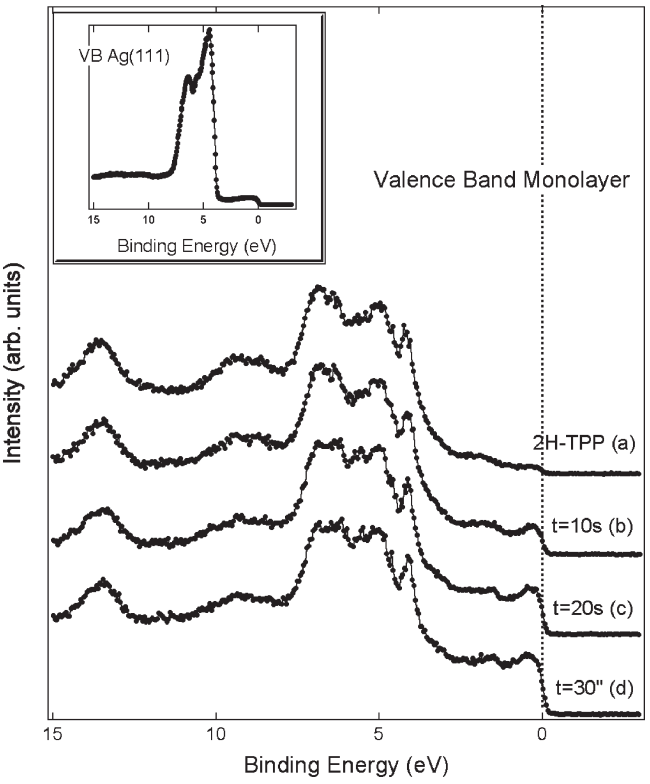

Figure 6. Valence band structures of one TPP monolayer. The sequence of the ML valence band spectra is raw data after subtraction of the valence band of clean Ag (inset) taken under the same conditions. The used photon energy was $h\nu$ = 175 eV.

metalation on Ag(111).[11] On this substrate, the 2H-TPP lies flat, both with macrocycle and phenyl rings, as the phtalocyanine. Therefore, the Fe metalation is probably not a substrate surface mediated process since the flat geometry leaves no space underneath the molecules for Fe diffusion as it would if the phenyls were rotated.

The metal coordination during the deposition of iron atoms can additionally be followed in the valence band region. Aiming for a better understanding of these spectra, we have compared the valence band data of the multilayer with those of the monolayer. Indeed, a parallel experiment has been done to directly obtain an Fe-TPP monolayer by thermal desorption of the corresponding Fe-TPP multilayer. In Figure 5, we report the valence band data of an Fe-TPP multilayer (a) and of one Fe-TPP monolayer obtained either by depositing Fe on a monolayer of 2H-TPP (b) or by the thermal desorption of the metalated Fe-TPP multilayer (c). The latter (c) almost completely matches the one obtained after the step-by-step Fe evaporation (b) indicating the reliability of the two methods. This also means an Fe-TPP desorption from the multilayer showing that the Fe-porphyrin bond is extremely stable and strong.

The sequence of the ML valence band spectra, shown in Figure 6, is raw data to which we have subtracted the valence band of the clean Ag surface collected in the same conditions. This procedure allows the direct visualization of molecular orbitals and modified substrate features as long as the metal coordination takes place without the strong background of the metallic substrate (Ag 4d at BE = 4.5eV and Ag Fermi edge as shown in the inset of Figure 6). New features near the Fermi level edge appear, and they smoothly increase with Fe deposition, indicating an overlap between the Fe and the Ag bands in that region. The main change in these spectra is the presence of a new highest occupied molecular orbital (HOMO) band that crosses the Fermi level, and the intensity increases as the iron binds to the macrocycle. Considering that the subtraction excludes any effect coming from the flat and much less intense sp bands of the clean substrate, the growth of the peak near the Fermi level is due to the d orbitals of the iron. These Fe d states near the Fermi level are expected to have much less hybridization with the N states. Instead, the possible hybridization between the perpendicular d orbitals (i.e., the d_{z^2}) and the silver states should enhance the charge-transfer process from the substrate to the molecules.

Moreover, the visualization of the valence bands is also important for monitoring the Fe adatom dosing on the molecular layer. Actually, an excess of Fe because of clusterlike deposition would have immediately resulted in a stronger peak located at the Fermi edge in comparison with the molecular features, which has not been noticed in this case (see Supporting Information).

To deepen the analysis of the multilayer valence bands, we show in Figure 7 the sequence of spectra measured during the metalation. The effect of the Fe coordination is followed in Figure 7 (bottom panel) where the reported valence band has been obtained by subtracting the spectrum of the 2H-TPP multilayer from the valence band after each evaporation step. This procedure highlights the molecular changes during the Fe atom coordination. The major changes are at BE below 7 eV and, in particular, there is a clear growth of states near the Fermi level and an apparent metallic behavior. To highlight the overlayer molecular features, considering that we have only four layers and that the Ag signal is dominant, in Figure 7 (upper panel), we have subtracted from each spectrum the valence band of the corresponding intermediate step obtained for the monolayer and reported in Figure 6. In this case, we assume that the monolayer metalation is, more or less, similar to the corresponding first layer

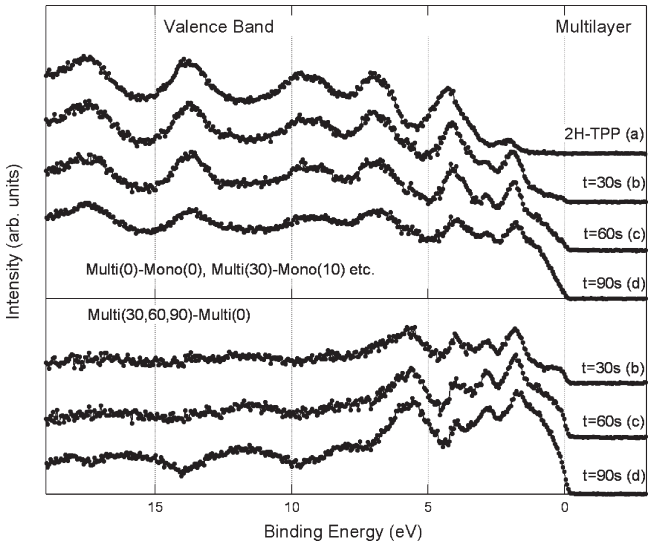

Figure 7. Valence band structure of a TPP multilayer. The used photon energy was $h\nu$ = 175 eV. The reported valence band has been obtained by (bottom panel) subtracting the spectrum of the 2H-TPP multilayer from the valence band after each evaporation step and (upper panel) by subtracting from each multilayer spectrum the valence band of the corresponding intermediate step taken for the monolayer.

metalation for the multilayer. This procedure obviously is quite rough but helps us to highlight some important features. The Fe metalation influences the states near the Fermi level (0−3 eV), but the layers above the first are nonmetallic with a density of states that goes almost linearly to zero at the Fermi level. Therefore, the intensity at the Fermi level seen in multilayer valence band is, instead, due to the metallization of the first monolayer. From the comparison between the spectra of Figure 7 and those of Figure 6, we conclude that the charge injection from the substrate is confined to the first monolayer.

From calculations, the Fe d states are expected to hybridize with the neighboring N p states in the energy range 0−5 eV below the Fermi level.[30] This is in agreement with our findings. The states from 4 to 7 eV are related to macrocycle σ orbitals, which according to the calculations have a small hybridization with Fe.

CONCLUSIONS

In-situ Fe atom coordination with tetraphenylporphyrin molecules has been successfully reproduced in UHV on Ag(111) by following an already known recipe.[10] An extensive surface characterization by means of XPS, valence band photoemission, and NEXAFS with synchrotron radiation light has followed the subsequent coordination steps for the monolayer and multilayer cases.

The NEXAFS spectra, taken in s and p light polarization at N and C K-edges, put in evidence the flat configuration for the macrocycle and showed that the phenyl groups lie flat in the case of the monolayer while having nonflat orientation in the multilayer. The multilayer Fe metalation favors a macrocycle N distortion, while in the monolayer, the conformation of the phenyl legs and the interaction with the substrate reduce the degrees of freedom of the macrocycle toward the already reached lowest energy situation. The influence of the Fe metallic center in the porphyrin core has only minor structural effects in the monolayer. The macrocycle Fe−N bonding is strong enough to allow the sublimation of the Fe-TPP multilayer at 530 K leaving the Fe-TPP monolayer. From the electronic point of view, the monolayer showed a metallic behavior despite the small Fe atom concentration as confirmed by the Doniach−Sunjic asymmetry parameter in the XPS fitting functions. Both core level and valence band photoemission results give evidence that the charge injection from the substrate is more likely confined to the first monolayer. The metallic state of the first layer evolves with Fe complexation because of d state hybridization with the s−p bands of the substrate.

The geometrical adaptation of the molecules in the monolayer has implications on the possible hypothesis for the metalation mechanism. A simple adatom hopping instead of a substrate surface mediated dopant diffusion to the reaction sites explains the metalation process. Alternatively, the iron atoms might be incorporated within the surface layers and diffused via atom exchange.

ASSOCIATED CONTENT

Supporting Information. Additional data collected during the experiments. This material is available free of charge via the Internet at http://pubs.acs.org.

AUTHOR INFORMATION

Corresponding Author
*E-mail: andrea.goldoni@elettra.trieste.it.

REFERENCES

(1) Scudiero, L.; Barlow, D. E.; Mazur, U.; Hipps, K. W. *J. Am. Chem. Soc.* **2001**, *123*, 4073–80.
(2) Baciocchi, E.; Lanzalunga, O.; Lapi, A.; Manduchi, L. *J. Am. Chem. Soc.* **1998**, *120*, 5783–5787.
(3) Woehrle, D. *J. Porphyrins Phthalocyanines* **2000**, *4*, 418–424.
(4) Gambardella, P.; Stepanow, S.; Dmitriev, A.; Honolka, J.; Groot, F. M. F. D.; Gupta, S. S.; Sarma, D. D.; Bencok, P.; Stanescu, S.; Clair, S.; Lin, N.; Seitsonen, A. P.; Brune, H.; Barth, J. V.; Kern, K. *Nat. Mater.* **2009**, *8*, 189–193.
(5) Williams, F. J.; Vaughan, O. P. H.; Knox, K. J.; Bampos, N.; Lambert, R. M. *Chem. Commun. (Cambridge, U.K.)* **2004**, *44*, 1688–1689.
(6) Buchner, F.; Schwald, V.; Comanici, K.; Steinrück, H.-P.; Marbach, H. *ChemPhysChem: Eur. J. Chem. Phys. Phys. Chem.* **2007**, *8*, 241–243.
(7) Weber-Bargioni, A.; Reichert, J.; Seitsonen, A. P.; Auwärter, W.; Schiffrin, A.; Barth, J. *J. Phys. Chem. C* **2008**, *112*, 3453–3455.
(8) Buchner, F.; Flechtner, K.; Bai, Y.; Zillner, E.; Kellner, I.; Steinrück, H.-P.; Marbach, H.; Gottfried, J. M. *J. Phys. Chem. C* **2008**, *112*, 15458–15465.
(9) Kretschmann, A. M.-M.; Walz, M.; Flechtner, K.; Steinrück, H.-P.; Gottfried, J. *Chem. Commun.* **2007**, 568–570.
(10) Gottfried, J. M.; Flechtner, K.; Kretschmann, A.; Lukasczyk, T.; Steinrück, H.-P. *J. Am. Chem. Soc.* **2006**, *128*, 5644–5645.
(11) Bai, Y.; Buchner, F.; Wendahl, M.; Kellner, I.; Bayer, A.; Steinrück, H.-P.; Marbach, H.; Gottfried, J. *J. Phys. Chem. C* **2008**, *112*, 6087–6092.
(12) Fukuzumi, S. *J. Porphyrins Phthalocyanines* **2000**, *4*, 398–400.
(13) Shubina, T. E.; Marbach, H.; Flechtner, K.; Kretschmann, A.; Jux, N.; Buchner, F.; Steinrück, H.-P.; Clark, T.; Gottfried, J. M. *J. Am. Chem. Soc.* **2007**, *129*, 9476–9483.
(14) Lukasczyk, T.; Flechtner, K.; Merte, L.; Jux, N.; Maier, F.; Gottfried, J.; Steinrück, H.-P. *J. Phys. Chem. C* **2007**, *111*, 3090–3098.

(15) Auwärter, W.; Weber-Bargioni, A.; Brink, S.; Riemann, A.; Schiffrin, A.; Ruben, M.; Barth, J. V. *ChemPhysChem: Eur. J. Chem. Phys. Phys. Chem.* **2007**, *8*, 250–254.
(16) Floreano, L.; Naletto, G.; Cvetko, D.; Gotter, R.; Malvezzi, M.; Marassi, L.; Morgante, A.; Santaniello, A.; Verdini, A.; Tommasini, F.; Tondello, G. *Rev. Sci. Instrum.* **1999**, *70*, 3855.
(17) Floreano, L.; Cossaro, A.; Gotter, R.; Verdini, A.; Bavdek, G.; Evangelista, F.; Ruocco, A.; Morgante, A.; Cvetko, D. *J. Phys. Chem. C* **2008**, *112*, 10794–10802.
(18) Zangrando, M.; Zacchigna, M.; Finazzi, M.; Cocco, D.; Rochow, R.; Parmigiani, F. *Rev. Sci. Instrum.* **2004**, *75*, 31.
(19) Stöhr, J. *NEXAFS Spectroscopy*; Springer: Berlin, 1992.
(20) Polzonetti, G. *Chem. Phys.* **2004**, *296*, 87–100.
(21) Castellarin-Cudia, C.; Borghetti, P.; Di Santo, G.; Fanetti, M.; Larciprete, R.; Cepek, C.; Vilmercati, P.; Sangaletti, L.; Verdini, A.; Cossaro, A.; Floreano, L.; Morgante, A.; Goldoni, A. *ChemPhysChem* **2010**, *11*, 2248–2255.
(22) Eichberger, M.; Marschall, M.; Reichert, J.; Auwärter, W. *NANO* **2008**, *8*, 4608–4613.
(23) Moresco, F.; Meyer, G.; Rieder, K.-h.; Ping, J.; Tang, H.; Joachim, C. *Surf. Sci.* **2002**, *499*, 94–102.
(24) Di Santo, G.; Blankenburg, S.; Castellarin-Cudia, C.; Fanetti, M.; Borghetti, P.; Sangaletti, L.; Floreano, L.; Alberto Verdini, A.; Magnano, E.; Bondino, F.; Pignedoli, C. A.; Nguyen, M.-T.; Gaspari, R.; Passerone, D.; Goldoni, A. submitted.
(25) Sarkar, D. K.; Zhou, X. J.; Tannous, A.; Louie, M.; Leung, K. T. *Solid State Commun.* **2003**, *125*, 365–368.
(26) Aue, D. H.; Webb, H. M.; Bowers, M. T. *J. Am. Chem. Soc.* **1975**, *97*, 4136–4137.
(27) Krasnikov, S. A.; Sergeeva, N. N.; Brzhezinskaya, M. M.; Preobrajenski, A. B.; Sergeeva, Y. N.; Vinogradov, N. A.; Cafolla, A. A.; Senge, M. O.; Vinogradov, A. S. *J. Phys.: Condens. Matter* **2008**, *20*, 235207.
(28) Poveda, L. A.; Ferro, V. R.; García de la Vega, J. M.; González-Jonte, R. H. *Phys. Chem. Chem. Phys.* **2000**, *2*, 4147–4156.
(29) Doniach, S.; Sunjic, M. *J. Phys. C: Solid State Phys.* **1970**, *285*, 285–291.
(30) Panchmatia, P.; Sanyal, B.; Oppeneer, P. *Chem. Phys.* **2008**, *343*, 47–60.
(31) Auwärter, W.; Seufert, K.; Klappenberger, F.; Reichert, J.; Weber-Bargioni, A.; Verdini, A.; Cvetko, D.; Dell'Angela, M.; Floreano, L.; Cossaro, A.; Bavdek, G.; Morgante, A.; Seitsonen, A. P.; Barth, J. V. *Phys. Rev. B* **2010**, *81*, 1–14.
(32) Bai, Y. PhD thesis, Friedrich-Alexander-Universität Erlangen-Nürnberg, Germany, 2010.